Comparison of Polarization Energies from B3LYP and MP2 Parameterizations: Spherical Benzene and Anthracene Clusters

Thomas T. Testoff and Lichang Wang*

School of Chemical and Biomolecular Sciences

Southern Illinois University Carbondale, Carbondale, IL 62901, USA

Abstract

To characterize polarization energies of organic small molecule based materials induced by aggregation, electronic structure calculations including density function theory (DFT) method become intractable when the size of the aggregates increases. A practical solution is to develop force field based on electronic structure calculations and molecular dynamics simulations. In this work, we performed B3LYP and MP2 calculations of neutral, cationic, and anionic benzene and anthracene and used these results to derive the state specific atomic polarizabilities (SSAPs) then to calculate the atomic dipole moments using QTAIM for better parameterization of the isotropic atomic polarizability for ionic systems. Ren's atomic multipole parameterization method was also compared to a less computationally intensive B3LYP result and a grid quadrature method for multipole analysis in GDMA. Our results show that the trend in cluster size is the same for both parameterization methods, however, the magnitude of the apparent polarization energy is different for the bulk with a negatively charged carrier. B3LYP produces results closer to the experimental values for the positively charged carrier. The intramolecular electrostatic interactions of the negative charge carrier are a major depolarizing force. This relationship is reversed in the positive charge carrier.

* Corresponding author: lwang@chem.siu.edu

1. Introduction

Organic small molecule (OSM) based materials have been widely used in many applications, such as in the fields of energy[1-18] and sensing,[19-36] due to their abundance and versatility of functionalization that makes systematically tuning device performance feasible. As such, studies of organic small molecules have become a very active research field ranging from designing special functionalities,[37-57] studying the excited state properties of OSMs,[58-77] to synthesis of OSMs[78-103] and the OSM aggregates.[104-106] As many of the device performances depend critically on the properties of aggregates,[3,107-130] studies of the effect of aggregation on electronic properties have become an important research frontier. Although computational studies of the aggregate effects play an important role in our understanding of aggregation effect, the challenge of such computational studies comes from the size effect. When the size of aggregate increases, electronic structure calculations, which will be a choice of method, become prohibitive. Alternative methods are therefore actively explored.

The apparent polarization (W) is a measurable quantity defined as the difference between the ionization potential or electron affinity in the solid vs vacuum state. (Fig. 1.) Through Koopman's theorem it can be seen how this is particularly important for the calculation of the total band energy splitting of small organic molecules. Specifically, the relation of IP and EA to the HOMO and LUMO respectively, directly correlates to how excitonic energy splitting in a bulk would lower the band gap.[131] This accounts for the aggregation effects seen in organic thin films which are red-shifted in comparison to the single molecule calculations often used as computational support. This is particularly important for computationalist looking to examine promising materials for OPVs. Molecular systems whose aggregative conformations effect the band gap edge more

positively, further red-shifted, and induce greater charge carrier transport will allow for better selection of materials for thin films.[132-134]

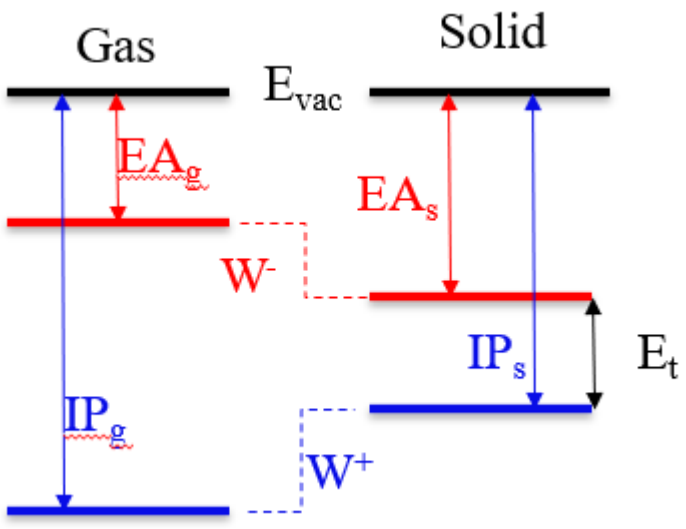

Figure 1. Energy diagram of the change in electron affinity (EA) and ionization potential (IP) between single molecule in vacuum and solid phase. The difference between the IP and EA between single molecule and solid phase is termed as the apparent polarization energy ($W^{+/-}$), respectively.

The magnitude of the apparent polarization that determines the IP and EA values in the bulk solid are also closely related to electron and hole transport. The transport gap, the energy required to make to independent charge carries infinitely separated in the bulk, is the difference in the bulk IP and EA values. Additionally, the binding energy of the exciton and the charge transfer exciton (CTE) energy play a role in free charge carriers.[131,135-137]

While periodic QM calculations serve their purpose in studying many of the crystalline films, amorphous materials still are difficult to study from a purely QM standpoint.[138,139] Additionally, nano-materials have garnered interest in OPVs of late and have shown promising effects on the power conversion efficiency. In the nanomaterial and disordered solid regimes where periodic plane-wave QM becomes difficult, most other QM methods become too computationally costly.

In this regime, QM/MM and MM calculations provide a substitute. Molecular Mechanic force fields have become well developed and have shown to be able to calculate the polarization energy and other electronic properties.[140-144] The AMOEBA force field in particular has been shown to give relatively accurate apparent polarization energies. AMOEBA is a good choice as it has explicit polarization terms that take into account the orientation and direction of the molecules in the solid through explicit multipole and induced dipole interactions. [145,146]

Recently, Xu et al. has shown that induced dipole interactions can be parameterized using QM based calculations where the parameter set of AMOEBA provided by Ren will be insufficient. Xu calculates the AMOEBA potential using state specific atomic polarizabilities based upon QM calculations of the neutral and ionic systems under a field. Combined with the electron density analysis from quantum theory of atom in molecules (QTAIM) by Bader, the change in the atomic multipole moments under electric field strengths can be used to parameterize the isotropic atomic polarizability. SSAPs provide a QM sensitive, species specific method to produce the isotropic atomic polarizability needed to calculate the polarization energy.[147-150]

Utilization of SSAPs and previously published extrapolation methods, will allow for calculation of the polarization energy of the positively and negatively charged ion. Additionally, MM methods allow for specification of the SSAPs and multipoles for individual molecules. By assigning the SSAP and multipole tensors to specific molecules the polarization energy of surface bulk vs infinite bulk can be compared. Additionally, Ren's parameterization method requires electrostatic fitting at the MP2/aug-cc-pvtz level in addition to MP2/6-311G(d,p) calculations. MP2 is already more exorbitant in computational cost then DFT and the aug-cc-pvtz basis set drastically increases calculation cost for the simplest molecules.

Herein, the small cyclic aromatic hydrocarbons, benzene and anthracene, are examined. The x-ray crystallographic structure (XRC) of each species was used to generate clusters of various size. The clusters energy was then calculated utilizing the AMOEBA force field under neutral and ionic conditions with SSAP parameterization. The bulk polarization energy was extrapolated by relating the inverse number of molecules per cluster to the apparent polarization energy. Ionic charge assignments were both placed centrally in the cluster. The results will serve as a foundation for future molecular dynamics studies[151,152] of the formation of aggregates from these molecules.

2. Methods

2.1 AMOEBA and Extrapolated Polarization

The AMOEBA polarizable force field was first produced in order to properly model water using molecular mechanics while directly treating polarization. The direct account of polarization through the explicit electrostatic and polarization terms allow for a direct calculation of bulk polarization energy by extrapolation.[146,153] Specifically, by drawing a relationship between the inverse of the number of molecules cubed of a cluster to the polarization energy, the infinite bulk value of the polarization energy and the apparent polarization energy can be obtained.[147,150]

Polarization is the difference in free energy between ionic and neutral molecules from vacuum to solid phase, as such the source of the free energy change is the difference in intermolecular interactions between each state. The difference in intermolecular interaction energy arises from three particular contributors: electrostatic interaction (multipole interactions), electrostatic polarization interactions (induced dipole interactions), and dispersion. [Eq. (1)] Each particular contributor to the apparent polarization ($\Delta E^{pol}, \Delta E^{es}, and\ \Delta E^{dis}$) are the difference in the change of ion when moving from bulk top solid with that of the neutral species. [Eq.(2)]

$$W^{+/-} = \Delta E^{es} + \Delta E^{pol} + \Delta E^{dis} \quad (1)$$

$$\Delta E^{pol} = \left(E^{pol}_{bulk,ion} - E^{pol}_{gas,ion}\right) - \left(E^{pol}_{bulk,neu} - E^{pol}_{gas,neu}\right) \quad (2)$$

Dispersion in AMOEBA is calculated as a 14—7 function, which Ponder describes as having a 'softer' repulsive region than a Lennard-Jones function and is the most suited to replicate gas phase ab initio results. This term is based on the potential well depth and radial distances between atom pairs. As the structures used to calculate the polarization energy are the geometrically the same between neutral and ionic species the radial values will not change, nor will the potential well depth, as the atom types will remain the same in the parameter set. As such the dispersion energy will be the same. This is indicative of two things: first, that any system where dispersion is significantly different between ionic bulk and neutral bulk application of AMOEBA will be inaccurate; second, polarization calculated by AMOEBA arises solely, from the multipole and induced dipole terms. For benzene and anthracene, the difference in dispersion energy should be much weaker than that of their electrostatic interactions, as such AMOEBA should be a suitable model.

$$E^{es} = \sum_i \sum_{j \neq i} M_i^T T_{ij} M_j \quad (3)$$

$$E^{pol} = \frac{1}{2} \sum_i \sum_{j \neq i} \mu_i^{ind} \cdot F_{j \to i} + \mu_j^{ind} \cdot F_{i \to j} \quad (4)$$

$$\mu_i^{ind} = \alpha_i \left(\sum_{mutual} T^{\alpha}_{i,mutual} M_j + \sum_{direct} T^{\alpha\beta}_{i,direct} \mu^{ind}_{direct,\beta} \right) \quad (5)$$

The explicitly treated multipole and induced dipole terms can be found in equation (3) and (4). The induced dipole of the ith atomic moment can be found in equation (5). The atomic multipole tensor of the ith atom (M_j) accounts for the charge, dipole, and quadrupole moments. T_{ij} is the atomic multipole interaction matrix defined by Stone. μ_i^{ind} is the atomic induced dipole moment, α_i is the isotropic atomic polarizability, and $F_{j\to i}$ is the electric field felt by the ith atom being produced by the multipoles of the jth. The term within the parenthetical of equation (4) is the summation of all fields felt by the ith atom from the static atomic multipoles of all other atoms. The first term within the parenthetical of equation (4) is the summation of the fields generated by the AMPs, while the second are those generated from induced dipole interactions. As equation 4 contains itself, AMOEBA must be solved self consistently through iteration. Thole's damping model was utilized to stop 'polarization catastrophe. The thole damping values were set to 0.39.[154,155]

Three different models were used to interpret the summation terms. In the first interpretation, the ith summation term in equations (3) and (4) is over all atoms within the ionic molecule and j is over all atoms not contained within the ion. This method characterizes solely the intermolecular interactions between the ionic molecule and its surroundings. We denote this as the intermolecular method. The second interpretation's ith term also only sums over the ionic molecule, while the jth term sums over all atoms that are not the ith atom. This accounts for not only the inter molecular interaction between the ion and its surroundings, but also the intramolecular interaction within the ion itself. This is to be termed as 'intra+inter' model. In the last interpretation, ith and jth summation both sum over all atoms, excluding atoms interacting with themselves and those whose values are scaled to 0 by the AMOEBA model. The AMOEBA model scales bonded neighbor interactions based upon the number of bonds between atoms. Additionally, the model has no

polarization within a polarization group; the groups in this instance are each individual molecule. This method is denoted as the 'full' model as it not only takes into account the ionic molecules interaction with its surroundings, but the changes in the interaction energies of the surrounding molecules with one another.

Atomic Multipoles were generated using Stone's GDMA 2.3.[149,156] The neutral single molecule structures were optimized using the 6-31+G(d,p) basis set and the B3LYP functional as well as at the MP2 level using the 6-311G(d,p) basis set .[157] Basis sets and functionals were chosen in accordance with previous research indicating that the Gauss-Hermite Quadrature works well for producing AMPS for functionals without diffuse functions whereas the grid based quadrature was suitable for diffuse functions.[158] As such the grid-based quadrature was utilized for the 6-31+G(d,p) basis set and the B3LYP functional while the Gauss-Hermite Quadrature was utilized for MP2/6-311G(d,p). Grid Based quadrature is activated using the 'SWITCH' command in GDMA. All GDMA calculations were done using the command SWITCH 2, indicating that the grid based quadrature was to be used up to the quadrupole values.

Ionic species were calculated from the optimized neutral geometries using the same basis set and functional. MP2/aug-cc-pvtz was used to optimize the neutral molecule further and then based upon this geometry calculate the MP2 density of the Neutral, Anionic and Cationic Species for electrostatic potential fitting. The electrostatic potential fitting gradient was set to 0.1. All QM calculations were done in Gaussian 16. AMOEBA calculations were run in Tinker 8.0 on crystal structures of benzene and anthracene determined by XRC.[159] As done by Xu et al., the mutual set stands for all atoms not contained within the same molecule as the ith atom and the direct set stands for all atoms that are not the ith atom. Atomic charges for each ion species were placed at the

center of the sphere, or on various parts of the surface. The charge transfer exciton was represented by placing a positively charge ion at the molecule closest to the center of mass of the cluster.[147]

2.2 State Specific Atomic Polarizabilities

As pointed out by Xu et al., there are three main limitations to the isotropic atomic polarizabilities produced by the parameterization done by Ren. First, the values produced do not characterize extended conjugated systems well. This is due to the particular set of training systems used to parameterize the aromatic carbon and hydrogen polarizabilities and the need to represent all aromatics, no matter how extended the conjugation may be, to one specific numeric representation. Second, the values of the open-shelled ions are greater than neutral polarizabilities. Lastly, atoms commonly used in organic aromatic systems, such as S, N, F are not parameterized for. Here, the second issue raised is of primary importance. As such, the QM-based state specific atomic polarizabilities (SSAPs) have been adopted.[147]

Atomic polarizability is the tendency for an atomic dipole to change under the influence of an electric field. In the bulk, something tantamount to an electric field is produced by the surrounding molecule's AMPS. This field felt by the individual atoms induces a change in the atomic dipole based upon each individual atom's susceptibility to it. More fundamentally, the change in this dipole is caused by the change in the electron density and charge distribution within the molecule. The relationship of atomic properties to their electron density is the fundamental basis of the application of the quantum theory of atoms in molecules (QTAIM). Bader proposed the use of QTAIM with a hard-space partitioning to calculate the molecular and atomic polarizability.

$$\alpha_A^{lm} = \lim_{F \to 0} \frac{u_{l,+m} - u_{l,-m}}{2F_m} \quad (6)$$

$$\alpha_A^{iso} = \frac{1}{3} \sum_{l=m} \alpha_{A,lm} \quad (7)$$

The SSAPs of benzene and anthracene are calculated using Keith's implementation of Bader's hard-space partitioning of polarizability in AIMALL. QM calculations to generate the electron density for basin analysis were completed using single point calculations on the B3LYP/631+G(d,p) optimized geometries at the CAM-B3LYP at the 6-311+G(d,p) level.[160] Calculations were done for the neutral, anionic, and cationic species under small electric fields of .005 a.u. in each cartesian direct (+x,-x,+y,-y,+z,-z) in Gaussian 16.[161,162] The atomic polarizability tensors were then found using symmetric numeric differentiation. [Eq. (6)] α_A^{lm} is the isotropic atomic polarizability of atom A in the **l** direction under the influence of an electric field in the **m** direction. F_m is the field strength in the **m** direction and $u_{l,+m}$ is the atomic dipole in the **l** direction under the influence of an electric field in the **m** direction. The isotropic atomic polarizability was then solved by averaging the trace of the polarizability tensor. [Eq. (7)] The resulting scalar value was scaled by 1.4 to reproduce the molecular polarizability as shown by Machi.

3. Results and Discussion

3.1 Apparent Polarization Energy

The apparent polarization energy is the measurable energy of change between gaseous and crystal state of the ionization potential (IP) and electron affinity (EA). This value is directly measurable by photo electron spectroscopy. According to equation (1) and Fig. 1 is the total sum

of change in the electrostatic, induced dipole, and Van der Waals energy between the ionic and neutral state from gaseous state to that of the bulk. The extrapolated bulk apparent polarization values can be found in Table 1. The apparent polarization values of each cluster and the regression lines can be seen in Figure 2. Results show that the cationic polarization energy of the purely intermolecular interactions between the cation and bulk has a similar energy value between the B3LYP and MP2 method for both benzene and anthracene.

Table 1. Summary of the theoretical apparent polarization ($W^{+/-}$), the induced dipole polarization ($P^{+/-/0}$), the contribution of the induced dipole polarization to the apparent polarization ($\Delta P^{+/-}$), the electrostatic energy from atomic multipole interactions($\Delta ES^{+/-}$), and the electrostatic contribution to the apparent polarization energy($\Delta ES^{+/-}$).

Molecule	Method	Model	W^+ (eV)	W^- (eV)	P^+ (eV)	P^- (eV)	P^0 (eV)	ΔP^+ (eV)	ΔP^- (eV)	ES^+ (eV)	ES^- (eV)	ES^0 (eV)	ΔES^+ (eV)	ΔES^- (eV)
Anthracene	MP2	Inter	1.33	1.29	1.08	1.66	0.11	0.97	1.55	0.74	0.13	0.38	0.36	-0.25
		w/ Intra	1.34	1.16	1.08	1.53	0.10	0.98	1.43	0.72	0.09	0.37	0.35	-0.26
		Full	1.25	1.24				0.88	1.52				0.35	-0.28
	B3LYP	Inter	1.35	0.94	1.02	1.43	0.11	0.91	1.32	0.89	0.08	0.47	0.42	-0.39
		w/ Intra	1.52	0.72	1.00	1.33	0.06	0.94	1.27	0.86	-0.26	0.29	0.57	-0.55
		Full	1.41	0.83				0.83	1.38				0.57	-0.56
	Lit		1.62[1]	1.09[1]										
Benzene	MP2	Inter	1.42	0.59	1.34	1.56	0.07	1.27	1.49	0.37	-0.68	0.21	0.16	-0.89
		w/ Intra	1.43	0.49	1.34	1.55	0.06	1.28	1.49	0.34	-0.81	0.19	0.15	-1.00
		Full	1.40	0.62				1.26	1.63				0.15	-1.00
	B3LYP	Inter	1.48	1.24	1.28	1.65	0.06	1.22	1.59	0.54	-0.07	0.27	0.27	-0.34
		w/ Intra	1.71	0.94	1.26	1.52	0.01	1.25	1.51	0.35	-0.81	-0.11	0.46	-0.70
		Full	1.64	1.01				1.18	1.57				0.46	-0.56
	Lit		1.59[3]	1.69[2]										

1 A. I. Belkindand and V. V. Grechov, Phys. Status Solidi A, 1974, 26, 377–384
2 Refaely-Abramson, S., Sharifzadeh, S., Jain, M., Baer, R., Neaton, J. B., and Kronik,L. (2013). Gap renormalization of molecular crystals from density-functional
theory. Phys. Rev. B 88:081204. doi: 10.1103/PhysRevB.88.081204
3 N. Sato, K. Seki, H. Inokuchi ***J. Chem. Soc., Faraday Trans. 2***, 1981,**77**, 1621-1633

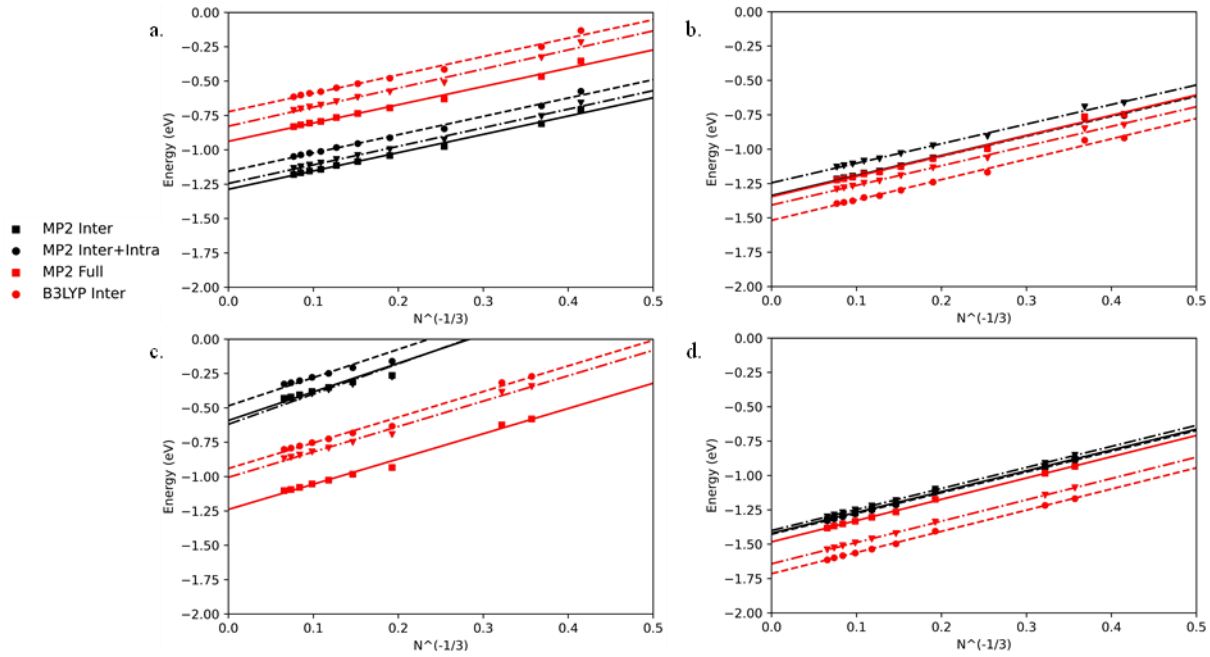

Figure 2. Apparent Polarization energy calculated using SSAPs as well as multipole parameters derived from the B3LYP (Red) and MP2 (Black). (a) Anthracene apparent polarization energy due to a negatively charged carrier (W^-) (b) Anthracene apparent polarization energy due to positively charged carrier (W^+) (c) Benzene apparent polarization energy due to a negative charge carrier (W^-) (d) Benzene apparent polarization energy due to a positive charge carrier (W^+)

The methods really differentiate themselves in regards to the intramolecular interactions of the ion. B3LYP has a much larger intramolecular energy due to its larger approximation of the atomic charge and dipole values. (Supporting Information) Additionally, the intramolecular B3LYP values increase the polarization, whereas the MP2 values are closer to zero or tend to depolarize (decrease polarization). The depolarization components, the environment-environment interactions and the intramolecular interactions of the environment, included in the full model have similar values of around 0.1 eV for anthracene. For benzene the cations environmental polarization is relatively similar in magnitude between functionals although only B3LYP predicts depolarization. Decreasing the magnitude of the total apparent polarization energy of the cation similar to what was found using the quantum patch method on NPB, TCTA and C_{60}.[143]

While B3LYP parameterization leads to a calculated value much closer to that of experiment for the polarization due to a positive charge carrier, the predicted values of the negative charge carrier has relatively similar error. However, the deviation between the predicted energy for B3LYP and MP2 is much larger. Interestingly, the intramolecular interaction of the negatively charged species for both molecules and functionals has the opposite contribution to the apparent polarization than it's positively charged counterpart suggesting that the AMOEBA model predicts the anion's intramolecular electrostatic to have a depolarization effect. Additionally, the environmental interactions are no longer depolarizing. The polarization contribution of the environment is also approximately 0.1 eV for the anion. The benzene anion has the largest difference in its apparent polarization energy possibly due to the larger RMS potential difference upon electrostatic fitting of MP2 to the aug-cc-pvtz basis set or drastically differing characterization of the anion electron density of the benzene system due to a mischaracterization of long range behavior by the exchange potential employed.[163]

From looking at the cluster energies themselves in Figure 2, it can be seen that the relative change in energy due to cluster size is equivalent for all models and methods employed. The change in energy per the cube root of the inverse number of molecules is the same resulting in nearly numerically identical slopes. This indicates that the cluster energy change is parameterization resistant, the exception being when the RMS potential fitting has exorbitantly large differences. It also implies that the induced dipole polarization values will be of similar magnitude for both methods. Since the dipole moments for both molecules are small to nonexistant, quadrupole interactions will play a predominate roll. As quadrupole interactions weaken with larger interatomic distance at a greater degree than dipoles, it's expected that the electrostatic energy should reach a value equivalent to the bulk at a relatively small cluster size.

Therefore, almost the entirety of the change in polarization between the cluster sizes should come from the induced dipole polarization.

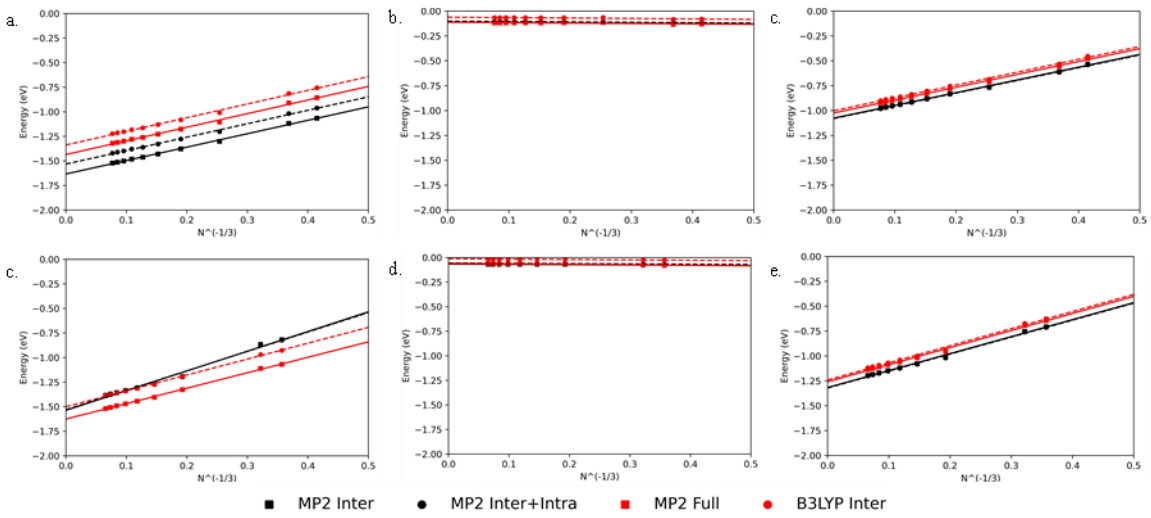

Figure 3. Polarization energy due to induced dipole interaction energy calculated using SSAPs as well as multipole parameters derived from the B3LYP (Red) and MP2 (Black). (a,b,c) Anthracene induced dipole polarization due to a negative, no , and positive charge carrier respectively. (P^-,P^0,P^+) (d,e,f) Benzene induced dipole polarization due to a negative, no , and positive charge carrier respectively. (P^-,P^0,P^+)
.

3.2 Induced Dipole Polarization and Electrostatic Energy

Breaking the apparent polarization down into its individual components it can be seen that for both benzene and anthracene the positive charge carrier induced dipole polarization is similar between MP2 and B3LYP (Figure 3. And Table 1). Additionally, the intramolecular induced dipole polarization contribution is minimal. This is to be expected as AMOEBA parameterization removes the molecular mechanics polarization from DMA using the isotropic atomic polarizability for the single molecule, and the bonded interactions are scaled such that atoms within two bond lengths do not 'feel' from one another. However, if the scalar SSAP values and the atomic multipoles are larger, such as in the negative charge carrying species, the intramolecular interaction is no longer insignificant(~0.1 eV). The induced dipole polarization energy of the positive, negative and neutral bulk all had decreasing or the same induced dipole polarization when

intramolecular interactions were included. The contribution to the apparent polarization energy increases by less than 0.05 eV for the bulk cluster with a positively charged carrier and experiences a small degree of depolarization from the negative charge carrier's intramolecular induced dipole contribution.

Looking at the 'Full' model the induced dipole environmental interactions play a predominate roll in the environmental contribution to the depolarization effect. This is further shown as there is no significant change in the bulk electrostatic energy between the 'intra+inter' and 'full model' (Figure 4. And Table S1). The diminishing effect of the ion's multipole strength over the radial distance between molecules suggests that this is likely due to the interactions between the nearest neighbors of the charge carrying molecule. The only exception to this is the benzene B3LYP negatively charged bulk in which ~2/3 of the environmental depolarization energy comes from the electrostatic multipole interaction. In contrast, the intramolecular interaction of the charge carrier largely contributes to the polarization of benzene through electrostatic multiple interactions. In anthracene, there is a clear distinction between the two models in this regard, as the electrostatic contribution of the intramolecular interactions of B3LYP (0.15 eV) is greater than that of MP2 (~0.01 eV). B3LYP in general has larger intramolecular electrostatic contributions, accounting for the vast majority of the difference between the two parameterization methods. It should be noted that this could be exacerbated by molecules with larger dipole moments.

Lastly, the electrostatic interaction of the anion is always depolarizing and the cation increases polarization. The intramolecular interaction of the cation likewise increases polarization and the anion depolarizes. The difference in sign of the electrostatic contribution of the anion and the cation is largely why the apparent polarization energy of the positively charged bulk is greater than

that of the negatively charge bulk despite having a smaller induced dipole contribution to the apparent polarization energy.

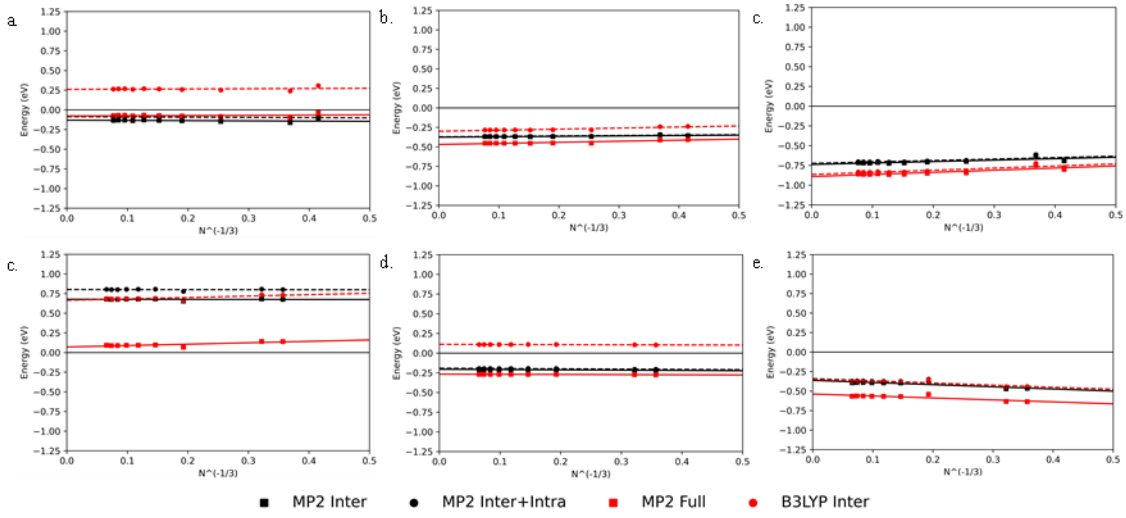

Figure 4. Electrostatic energy calculated using multipole parameters derived from the B3LYP (Red) and MP2 (Black). (a,b,c) Anthracene induced dipole polarization due to a negative, no , and positive charge carrier respectively. (ES^-,ES^0,ES^+) (d,e,f) Benzene induced dipole polarization due to a negative, no , and positive charge carrier respectively. (ES^-,ES^0,ES^+)

4. Conclusions

Herein, we have characterized benzene and anthracene's apparent polarization energy and the contributions the electrostatic and induced dipole interactions to the apparent polarization energy using the AMOEBA polarizable force field. The isotropic atomic polarizabilities were obtained using QTAIM analysis to generate the atomic multipoles of the ionic and neutral molecules under a field and symmetric numeric differentiation. These are referred to as state specific atomic polarizabilities. Atomic multipoles were generated using Anthony Stone's GDMA 2.3 and the electron density of the charged and neutral species calculated at both B3LYP/6-31+G(d,p) and MP2/6-311G(d,p) with electrostatic potential fitting at the MP2/aug-cc-pvtz level. The Gauss-Hermite quadrature method was used for MP2 while the grid based quadrature was used for B3LYP. Benzene and anthracene cluster of increasing size were constructed and ionic charges

placed at the molecule nearest the center of mass. Bulk apparent polarizabilities were then extrapolated by relating energy with the inverse of the cube root of the number of molecules. Induced dipole polarization and electrostatic multipole contribution were extrapolated similarly.

This work shows that while the change in energy between cluster sizes is nearly identical between B3LYP and MP2, the magnitude of the electrostatic multipole interactions plays a large role in the discrepancies between the extrapolated bulk energies. In particular, the intramolecular electrostatic interactions are larger in B3LYP owing to larger multipole moments. The bulk apparent polarization energy of the positive charge carrier is well reproduced, but the negative charge carrier has large variance between the two methods. Large differences in the electrostatic are not the only cause for this. The difference in the induced dipole polarization becomes significant owing to the larger SSAP values of the anion.

The intramolecular electrostatic interactions of the negative charge carrier are a major depolarizing force, while in the positive charge carrier it accounts for the majority of the increase in the intramolecular polarization. The environmental interactions have the opposite effect of the intramolecular interactions. Where the intramolecular interactions are depolarizing the environmental interaction contribute positively to the polarization and vice versa. The difference between the induced dipole polarization is insignificant, however, there is a slight difference in the neutral electrostatic polarization ($\leq$0.1 eV)

Utilization of B3LYP/6-31G(d,p) reduces computational costs significantly in parameterization and adequately captures the value of the bulk apparent polarization of the postively charged carrier's interaction with its surroundings. The increased polarization due to the intramolecular electrostatic interaction also better reproduces the experimental results. The magnitude of the bulk values of B3LYP for the negatively charged carrier vary wildly from MP2,

however, they still manage to capture the trend between changes in cluster size. Utilizing well tested functionals and a basis set with sufficient long range interaction may better characterize the negative charge carrier's electron density. Lastly, large RMS potential differences during electrostatic potential fitting should be considered carefully, this is the only instance where B3LYP parameterization produced a different trend then that of MP2.

Acknowledgements

Thomas Testoff acknowledges the support of the Gower Fellowship and the Doctoral Research Award, Southern Illinois University Carbondale.

References

(1) Feng, W.; Geng, R.; Liu, D.; Wang, T.; Testoff, T. T.; Li, W.; Hu, W.; Wang, L.; Zhou, X. *Org. Electronics* **2021**, *703*, 121742.

(2) Zheng, Y.; Chen, Y.; Cao, Y.; Huang, F.; Guo, Y.; Zhu, X. *ACS Mater. Lett.* **2022**, *4*, 882.

(3) Xu, F.; Gong, K.; Liu, D.; Wang, L.; Li, W.; Zhou, X. *Solar Energy* **2022**, *240*, 157.

(4) Wang, X.; Zhao, B.; Kan, W.; Xie, Y.; Pan, K. *Adv. Mater.* **2022**, *9*, 2101229.

(5) Venkatesan, S.; Hsua, T.-H.; Wong, X.-W.; Teng, H.; Lee, Y.-L. *Chem. Eng. J.* **2022**, *446*, 137349.

(6) Nicksonsebastin, D.; Pounraj, P.; Prasath, M. *J. Mol. Model.* **2022**, *28*, 102.

(7) Liraz, D.; Tesslera, N. *Chem. Phys. Rev.* **2022**, *3*, 031305.

(8) He, S.; Lan, Z.; Zhang, B.; Gao, Y.; Shang, L.; Yue, G.; Chen, S.; Shen, Z.; Tan, F.; Wu, J. *ACS Appl. Mater. Interfaces* **2022**, *14*, 43576.

(9) Ge, F.; Xu, F.; Gong, K.; Liu, D.; Li, W.; Wang, L.; Zhou, X. *Dyes Pigm.* **2022**, *200*, 110127.

(10) Sun, H.; Liu, D.; Wang, T.; Lu, T.; Li, W.; Ren, S.; Hu, W.; Wang, L.; Zhou, X. *ACS Appl. Mater. Interfaces* **2017**, *9*, 9880.

(11) Ni, M.-Y.; Leng, S.-F.; Liu, H.; Yang, Y.-K.; Li, Q.-H.; Sheng, C.-Q.; Lu, X.; Liu, F.; Wan, J.-H. *J. Mater. Chem. C* **2021**, *9*, 3826.

(12) Munoz-Garcia, A. B.; Benesperi, I.; Boschloo, G.; Concepcion, J. J.; Delcamp, J. H.; Gibson, E. A.; Meyer, G. J.; Pavone, M.; Pettersson, H.; Hagfeldt, A.; Freitag, M. *Chem. Soc. Rev.* **2021**, *50*, 12450.

(13) Kokkonen, M.; Talebi, P.; Zhou, J.; Asgari, S.; Soomro, S. A.; Elsehrawy, F.; Halme, J.; Ahmad, S.; Hagfeldt, A.; Hashmi, S. G. *J. Mater. Chem. A* **2021**, *9*, 10527.

(14) Huaulmé, Q.; Mwalukuku, V. M.; Joly, D.; Liotier, J.; Kervella, Y.; Maldivi, P.; Narbey, S.; Oswald, F.; Riquelme, A. J.; Anta, J. A.; Demadrille, R. *Nat. Energy* **2020**, *5*, 468.

(15) Arunkumar, A.; Shanavas, S.; Acevedo, R.; Anbarasan, P. M. *Opt. Quantum Electron.* **2020**, *52*, 164.

(16) Zhou, R.; Jiang, Z.; Yang, C.; Yu, J.; Feng, J.; Adil, M. A.; Deng, D.; Zou, W.; Zhang, J.; Lu, K.; Ma, W.; Gao, F.; Wei, Z. *Nat. Commun.* **2019**, *10*, 5393.

(17) He, X.; Yin, L.; Li, Y. *J. Mater. Chem. C* **2019**, *7*, 2487.

(18) Gong, J.; Sumathy, K.; Qiao, Q.; Zhou, Z. *Renew. Sust. Energy Rev.* **2017**, *68*, 234.

(19) Kumar, N. S.; Prasad, K. N. N.; Chandrasekhar, S.; Thipperudrappa, J. *Chem. Phys. Impact* **2023**, *6*, 100136.

(20) Liu, M.; Muleta, D. Y.; Yu, Z.; Wang, L.; Liu, D.; Wang, T.; Hu, W. *J. Mater. Chem. C* **2022**, *10*, 12249.

(21) Feng, W.; Zengji, Z.; Testoff, T. T.; Wang, T.; Yan, X.; Li, W.; Liu, D.; Wang, L.; Zhou, X. *Anal. Chim. Acta* **2021**, *1153*, 338278.

(22) Chen, Z.; Yang, L.; Xu, W.; Xu, F.; Sheng, J.; Xiao, Q.; Song, X.; Chen, W. *Anal. Chem.* **2023**, *95*, 3325.

(23) Zhao, J.; Zheng, X. *Front. Chem.* **2022**, *9*, 808957.

(24) Zhang, J.; Lan, T.; Lu, Y. *Annu. Rev. Anal. Chem.* **2022**, *15*, 151.

(25) Zhang, Y.; Mollick, S.; Tricarico, M.; Ye, J.; Sherman, D. A.; Tan, J.-C. *ACS Sens.* **2022**, *7*, 2338.

(26) Wang, Y.; Wang, X.; Ma, W.; Lu, R.; Zhou, W.; Gao, H. *Chemosensors* **2022**, *10*, 399.

(27) Li, J.; Dong, Y.; Wei, R.; Jiang, G.; Yao, C.; Lv, M.; Wu, Y.; Gardner, S. H.; Zhang, F.; Lucero, M. Y.; Huang, J.; Chen, H.; Ge, G.; Chan, J.; Chen, J.; Sun, H.; Luo, X.; Qian, X.; Yang, Y. *J. Am. Chem. Soc.* **2022**, *144*, 14351.

(28) Yu, H.; Alkhamis, O.; Canoura, J.; Liu, Y.; Xiao, Y. *Angew. Chem. Int. Ed.* **2021**, *60*, 16800.

(29) Tian, X.; Murfin, L. C.; Wu, L.; Lewis, S. E.; James, T. D. *Chem. Sci.* **2021**, *12*, 3406.

(30) S., K.; Sam, B.; George, L.; N, S. Y.; Varghese, A. *J. Fluoresc.* **2021**, *31*, 1251.

(31) Shin, Y.-H.; Gutierrez-Wing, M. T.; Choi, J.-W. *J. Electrochem. Soc.* **2021**, *168*, 017502.

(32) Guo, S.; Dai, W.; Chen, X.; Lei, Y.; Shi, J.; Tong, B.; Cai, Z.; Dong, Y. *ACS Materials Lett.* **2021**, *3*, 379−397.

(33) Cotugno, P.; Massari, F.; Aresta, A.; Zambonin, C.; Ragni, R.; Monks, K.; Avagyan, L.; Bottcher, J. *J. Chromatogr. A* **2021**, *1639*, 461920.

(34) McLoughlin, C. K.; Kotroni, E.; Bregnhøj, M.; Rotas, G.; Vougioukalakis, G. C.; Ogilby, P. R. *Sensors* **2020**, *20*, 5172.

(35) Ma, Z.; Li, J.; Lin, K.; Ramachandran, M.; Li, M.; Li, Y. *Anal. Chem.* **2020**, *92*, 12282.

(36) Strakova, K.; Assies, L.; Goujon, A.; Piazzolla, F.; Humeniuk, H. V.; Matile, S. *Chem. Rev.* **2019**, *119*, 10977.

(37) Nagaraju, N.; Kushavah, D.; Kumar, S.; Ray, R.; Gambhir, D.; Ghosh, S.; Pal, S. K. *Phys. Chem. Chem. Phys.* **2022**, *24*, 3303.

(38) Loong, H.; Zhou, J.; Jiang, N.; Feng, Y.; Xie, G.; Liu, L.; Xie, Z. *J. Phys. Chem. B* **2022**, *126*, 2441.

(39) Wang, T.; Weerasinghe, K. C.; Ubaldo, P. C.; Liu, D.; Li, W.; Zhou, X.; Wang, L. *Chem. Phys. Lett.* **2015**, *618*, 142.

(40) Kundu, S.; Bhattacharjee, S.; Lee, S.-C.; Jain, M. *J. Chem. Phys.* **2021**, *154*, 104111.

(41) Sil, M. C.; Chen, L.-S.; Lai, C.-W.; Chang, C.-C.; Chen, C.-M. *J. Mater. Chem. C* **2020**, *8*, 11407.

(42) Yashwantrao, G.; Saha, S. *Dyes Pigm.* **2022**, *199*, 110093.

(43) Yao, H.; Ye, L.; Zhang, H.; Li, S.; Zhang, S.; Hou, J. *Chem. Rev.* **2016**, *116*, 7397.

(44) Wang, T.; Zhao, C.; Zhang, L.; Lu, T.; Sun, H.; Bridgmohan, C. N.; Weerasinghe, K. C.; Liu, D.; Hu, W.; Li, W.; Zhou, X.; Wang, L. *J. Phys. Chem. C* **2016**, *120*, 25263.

(45) Li, S.; Ye, L.; Zhao, W.; Zhang, S.; Mukherjee, S.; Ade, H.; Hou, J. *Adv. Mater.* **2016**, *28*, 9423.

(46) Hadmojo, W. T.; Nam, S. Y.; Shin, T. J.; Yoon, S. C.; Jang, S.-Y.; Jung, I. H. *J. Mater. Chem. A* **2016**, *4*, 12308.

(47) Agnihotri, N. *Chem. Phys. Lett.* **2016**, *665*, 40.

(48) Zhu, X.; Yuan, B.; Plunkett, K. N. *Tetrahedron Lett.* **2015**, *56*, 7105.

(49) Ni, W.; Li, M.; Liu, F.; Wan, X.; Feng, H.; Kan, B.; Zhang, Q.; Zhang, H.; Chen, Y. *Chem. Mater.* **2015**, *27*, 6077.

(50) Tao, Y.; Han, L.; Han, Y.; Liu, Z. *Spectrochim. Acta A* **2015**, *137*, 1078.

(51) Tarsang, R.; Promarak, V.; Sudyoadsuk, T.; Namuangruk, S.; Jungsuttiwong, S. *J. Photochem. Photobio. A: Chem.* **2014**, *273*, 8.

(52) Sumithra, M.; Sundaraganesan, N.; Rajesh, R.; Vetrivelan, V.; Ilangovan, V.; Javed, S.; Muthu, S. *Chem. Phys. Impact* **2023**, *6*, 100145.

(53) Wang, T.; Liu, M.; Gao, C.; Song, Y.; Wang, L.; Liu, D.; Wang, T.; Hu, W. *Dyes Pigm.* **2022**, *207*, 110734.

(54) Wang, R.; Gong, K.; Liu, R.; Liu, D.; Li, W.; Wang, L.; Zhou, X. *J. Porphyrins Phthalocyanines* **2022**, *26*, 469.

(55) Feng, W.; Wang, T.; Testoff, T. T.; Bridgmohan, C. N.; Zhao, C.; Sun, H.; Hu, W.; Li, W.; Liu, D.; Wang, L.; Zhou, X. *Spectrochim. Acta. Part A* **2020**, *229*, 118016.

(56) Weerasinghe, K. C.; Wang, T.; Zhuang, J.; Liu, D.; Li, W.; Zhou, X.; Wang, L. *Comput. Mater. Sci.* **2017**, *126*, 244.

(57) Wang, T.; Weerasinghe, K. C.; Liu, D.; Li, W.; Yan, X.; Zhou, X.; Wang, L. *J. Mater. Chem. C* **2014**, *2*, 5466.

(58) Manian, A.; Hudson, R. J.; Ramkissoon, P.; Smith, T. A.; Russo, S. P. *J. Chem. Theory Comput.* **2023**, *19*, 271.

(59) Gong, K.; Yang, J.; Testoff, T. T.; Li, W.; Wang, T.; Liu, D.; Zhou, X.; Wang, L. *Chem. Phys.* **2021**, *549*, 111256.

(60) Song, J.; Muleta, D. Y.; Feng, W.; Song, Y.; Zhou, X.; Li, W.; Wang, L.; Liu, D.; Wang, T.; Hu, W. *Dyes Pigm.* **2021**, *193*, 109501.

(61) Zhou, Q.; Xu, M.; Feng, W.; Li, F. *J. Phys. Chem. Lett.* **2021**, *12*, 9455.

(62) Yücel, M. B.; Sari, H.; Duque, C. M.; Duque, C. A.; Kasapoglu, E. *Int. J. Mol. Sci.* **2022**, *23*, 11429.

(63) Zhou, X.; Liu, D.; Wang, T.; Hu, X.; Guo, J.; Weerasinghe, K. C.; Wang, L.; Li, W. *J. Photochem. Photobiol. A: Chem.* **2014**, *274*, 57.

(64) Walkup, L. L.; Weerasinghe, K. C.; Tao, M.; Zhou, X.; Zhang, M.; Liu, D.; Wang, L. *J. Phys. Chem. C* **2010**, *114*, 19521.

(65) Wang, T.; Weerasinghe, K. C.; Sun, H.; Hu, X.; Lu, T.; Liu, D.; Hu, W.; Li, W.; Zhou, X.; Wang, L. *J. Phys. Chem. C* **2016**, *120*, 11338.

(66) Wu, R.; Wang, L. *Chem. Phys. Lett.* **2017**, *678*, 196.

(67) Miao, B.; Wu, Z.; Xu, H.; Zhang, M.; Chen, Y.; Wang, L. *Chem. Phys. Lett.* **2017**, *688*, 92.

(68) Wu, R.; Wang, L. *J. Phys. Chem. C* **2020**, *124*, 26953.

(69) Wu, C.; Wang, L.; Xiao, Z.; Li, G.; Wang, L. *Phys. Chem. Chem. Phys.* **2020**, *22*, 724.

(70) Wu, R.; Wang, L. *Comput. Mater. Sci.* **2021**, *196*, 110514.

(71) Wu, R.; Sun, K.; Chen, Y.; Zhang, M.; Wang, L. *Surf. Sci.* **2021**, *703*, 121742.

(72) Wu, R.; Wiegand, K. R.; Wang, L. *J. Chem. Phys.* **2021**, *154*, 054705.

(73) Wu, R.; Wang, L. *Chem. Phys. Impact* **2021**, *3*, 100040.

(74) Yang, J.; Liu, D.; Lu, T.; Sun, H.; Li, W.; Testoff, T. T.; Zhou, X.; Wang, L. *Int. J. Quantum Chem.* **2020**, *120*, e26355.

(75) Weerasinghe, K. C.; Wang, T.; Zhuang, J.; Sun, H.; Liu, D.; Li, W.; Hu, W.; Zhou, X.; Wang, L. *Chem. Phys. Impact* **2022**, *4*, 100062.

(76) Wang, T.; Sun, H.; Zhang, L.; Colley, N. D.; Bridgmohan, C. N.; Liu, D.; Hu, W.; Li, W.; Zhou, X.; Wang, L. *Dyes Pigm.* **2017**, *139*, 601.

(77) Lu, T.; Sun, H.; Colley, N. D.; Bridgmohan, C. N.; Liu, D.; Li, W.; Hu, W.; Zhou, X.; Wang, T.; Wang, L. *Dyes Pigm.* **2017**, *136*, 404.

(78) Pigulski, B.; Ximenis, M.; Shoyama, K.; Wuerthner, F. *Org. Chem. Front.* **2020**, *7*, 2925.

(79) Hwang, S.-H.; Choi, T.-L. *Org. Lett.* **2020**, *22*, 2935.

(80) Yin, H.; Ma, Y.; Lin, H.; Chen, S.; Zhou, Z.; Zhuo, S.; Wang, X. *Chin. J. Chem.* **2022**, *40*, 1149.

(81) Liu, J.; Li, X.; Zhang, L.; Liu, X.; Wang, X. *Carbon* **2022**, *188*, 453.

(82) Zhai, C.; Yin, X.; Niu, S.; Yao, M.; Hu, S.; Dong, J.; Shang, Y.; Wang, Z.; Li, Q.; Sundqvist, B.; Liu, B. *Nat. Commun.* **2021**, *12*, 4084.

(83) Hao, Y.; Li, Y.; Song, L.; Deng, Z. *J. Am. Chem. Soc.* **2021**, *143*, 3065.

(84) Dinleyici, M.; Al-Khateeb, B.; Abourajab, A.; Uzun, D.; Koyuncu, S.; Icil, H. *J. Photochem. Photobiol. A: Chem.* **2021**, *421*, 113525.

(85) Watanabe, H.; Takemoto, M.; Adachi, K.; Okuda, Y.; Dakegata, A.; Fukuyama, T.; Ryu, I.; Wakamatsu, K.; Orita, A. *Chem. Lett.* **2020**, *49*, 409.

(86) Pettipas, R. D.; Hoff, A.; Gelfand, B. S.; Welch, G. C. *ACS Appl. Mater. Interfaces* **2022**, *14*, 3103.

(87) Morioka, K.; Wakamatsu, K.; Tsurumaki, E.; Toyota, S. *Chem. Eur. J.* **2022**, *28*, e202103694.

(88) Li, J.; Ballmer, S. G.; Gillis, E. P.; Fujii, S.; Schmidt, M. J.; Palazzolo, A. M. E.; Lehmann, J. W.; Morehouse, G. F.; Burke, M. D. *Science* **2015**, *347*, 1221.

(89) Hammershøj, P.; Kumar, E. K. P.; Harris, P.; Andresen, T. L.; Clausen, M. H. *Eur. J. Org. Chem.* **2015**, *2015*, 7301.

(90) Azuma, E.; Kuramochi, K.; Tsubaki, K. *Tetrahedron* **2013**, *69*, 1694.

(91) Wu, C.; Wang, L.; Xiao, Z.; Li, G.; Wang, L. *Chem. Phys. Lett.* **2020**, *746*, 137229.

(92) Wu, R.; Wang, L. *J. Phys. Chem. C* **2022**, *126*, 21650.

(93) Wu, R.; Wang, L. *Phys. Chem. Chem. Phys.* **2023**, *25*, 2190.

(94) Wang, L.; Ore, R. M.; Jayamaha, P. K.; Wu, Z.-P.; Zhong, C.-J. *Faraday Discuss.* **2023**, *242*, 429.

(95) Wu, R.; Wang, L. *ChemPhysChem* **2022**, e202200132.

(96) Sun, K.; Zhang, M.; Wang, L. *Chem. Phys. Lett.* **2013**, *585*, 89.

(97) Lu, J.; Aydin, C.; Browning, N. D.; Wang, L.; Gates, B. C. *Catal. Lett.* **2012**, *142*, 1445.

(98) Wang, L.; Williams, J. I.; Lin, T.; Zhong, C. J. *Catal. Today* **2011**, *165*, 150.

(99) Xu, H.; Miao, B.; Zhang, M.; Chen, Y.; Wang, L. *Phys. Chem. Chem. Phys.* **2017**, *19*, 26210.

(100) Wu, Z.; Zhang, M.; Jiang, H.; Zhong, C.-J.; Chen, Y.; Wang, L. *Phys. Chem. Chem. Phys.* **2017**, *19*, 15444.

(101) Miao, B.; Wu, Z.-P.; Xu, H.; Zhang, M.; Chen, Y.; Wang, L. *Comput. Mater. Sci.* **2019**, *156*, 175.

(102) Wu, R.; Wiegand, K. R.; Ge, L.; Wang, L. *J. Phys. Chem. C* **2021**, *125*, 14275.

(103) Wu, C.; Xiao, Z.; Wang, L.; Li, G.; Zhang, X.; Wang, L. *Catal. Sci. Technol.* **2021**, *11*, 1965.

(104) Hu, G.; He, J.; Li, Y. *ACS Catal.* **2022**, *12*, 6712.

(105) Zhao, W.; He, Z.; Tang, B. Z. *Nat. Rev. Mater.* **2020**, *5*, 869.

(106) Chen, S.; Slattum, P.; Wang, C.; Zang, L. *Chem. Rev.* **2015**, *115*, 11967−11998.

(107) Parida, S.; Patra, S. K.; Mishra, S. *ChemPhysChem* **2022**, *23*, e202200361.

(108) Roosta, S.; Ghalami, F.; Elstner, M.; Xie, W. *J. Chem. Theory Comput.* **2022**, *18*, 1264.

(109) Zhang, Y.-Y.; Qiu, F.-Y.; Shi, H.-T.; Yu, W. *Chem. Commun.* **2021**, *57*, 3010.

(110) Tian, T.; Wei, D.; Ge, L.; Wang, Z.; Chen, C.; Guo, R. *J. Colloid Interface Sci.* **2021**, *601*, 746.

(111) Würthner, F.; Saha-Möller, C. R.; Fimmel, B.; Ogi, S.; Leowanawat, P.; Schmidt, D. *Chem. Rev.* **2016**, *116*, 962.

(112) Wang, X.; Song, P.; Peng, L.; Tong, A.; Xiang, Y. *ACS Appl. Mater. Interfaces* **2016**, *8*, 609.

(113) Liu, X.; Cole, J. M.; Chow, P. C. Y.; Zhang, L.; Tan, Y.; Zhao, T. *J. Phys. Chem. C* **2014**, *118*, 13042.

(114) Zhao, Z.; Chen, S.; Shen, X.; Mahtab, F.; Yu, Y.; Lu, P.; Lam, J. W. Y.; Kwok, H. S.; Tang, B. Z. *Chem. Commun.* **2010**, *46*, 686.

(115) Deshmukh, A. P.; Koppel, D.; Chuang, C.; Cadena, D. M.; Cao, J.; Caram, J. R. *J. Phys. Chem. C* **2019**, *123*, 18702.

(116) Bradbury, N. C.; Nguyen, M.; Caram, J. R.; Neuhauser, D. *J. Chem. Phys.* **2022**, *157*, 031104.

(117) Segalina, A.; Assfeld, X.; Monari, A.; Pastore, M. *J. Phys. Chem. C* **2019**, *123*, 6427.

(118) Chang, M.; Meng, L.; Wang, Y.; Ke, X.; Yi, Y.-Q.-Q.; Zheng, N.; Zheng, W.; Xie, Z.; Zhang, M.; Yi, Y.; Zhang, H.; Wan, X.; Li, C.; Chen, Y. *Chem. Mater.* **2020**, *32*, 2593.

(119) Fratini, S.; Mayou, D.; Ciuchi, S. *Adv. Funct. Mater.* **2016**, *26*, 2292.

(120) Li, Q.-Y.; Yao, Z.-F.; Wang, J.-Y.; Pei, J. *Rep. Prog. Phys.* **2021**, *84*, 076601.

(121) Ryno, S. M.; Risko, C.; Brédas, J.-L. *J. Am. Chem. Soc.* **2014**, *136*, 6421.

(122) Zhang, L.; Cole, J. M. *J. Mater. Chem. A* **2017**, *5*, 19541.

(123) Qin, S.; Meng, L.; Li, Y. *ACS Omega* **2021**, *6*, 14467.

(124) Chen, Z.; Li, W.; Zhang, Y.; Wang, Z.; Zhu, W.; Zeng, M.; Li, Y. *J. Phys. Chem. Lett.* **2021**, *12*, 9783.

(125) Sabuzi, F.; Stefanelli, M.; Monti, D.; Conte, V.; Galloni, P. *Molecules* **2020**, *25*, 133.

(126) Ang, S. T.; Pal, A.; Manzhos, S. *J. Chem. Phys.* **2018**, *149*, 044114.

(127) Testoff, T. T.; Aikawa, T.; Tsung, E.; Lesko, E.; Wang, L. *Chem. Phys.* **2022**, *562*, 111641.

(128) Liu, R.; Liu, D.; Meng, F.; Li, W.; Wang, L.; Zhou, X. *Dyes Pigm.* **2021**, *187*, 109135.

(129) Xu, F.; Gong, K.; Fan, W.; Liu, D.; Li, W.; Wang, L.; Zhou, X. *ACS Appl. Energy Mater.* **2022**, *5*, 13780.

(130) Xu, F.; Testoff, T. T.; Wang, L.; Zhou, X. *Molecules* **2020**, *25*, 4478.

(131) D'Avino, G.; Muccioli, L.; Castet, F.; Poelking, C.; Andrienko, D.; Soos, Z. G.; Cornil, J.; Beljonne, D. *Journal of Physics: Condensed Matter* **2016**, *28*, 433002.

(132) Sharma, K.; Sharma, V.; Sharma, S. S. *Nanoscale Research Letters* **2018**, *13*.

(133) Singh, R.; Giussani, E.; Mróz, M. M.; Di Fonzo, F.; Fazzi, D.; Cabanillas-González, J.; Oldridge, L.; Vaenas, N.; Kontos, A. G.; Falaras, P.; Grimsdale, A. C.; Jacob, J.; Müllen, K.; Keivanidis, P. E. *Organic Electronics* **2014**, *15*, 1347.

(134) Gao, M.; Wang, W.; Hou, J.; Ye, L. *Aggregate* **2021**, *2*.

(135) Bhardwaj, N. **2016**.

(136) Knupfer, M. *Applied Physics A* **2003**, *77*, 623.

(137) Zhu, L.; Yi, Y.; Wei, Z. *The Journal of Physical Chemistry C* **2018**, *122*, 22309.

(138) Stachurski, Z. H. *Materials* **2011**, *4*, 1564.

(139) Biswas, P.; Tafen, D. N.; Inam, F.; Cai, B.; Drabold, D. A. *Journal of Physics: Condensed Matter* **2009**, *21*, 084207.

(140) Gehan, T. S.; Ellis, C. L. C.; Venkataraman, D.; Bag, M. *ACS Applied Materials & Interfaces* **2020**, *12*, 8183.

(141) Xie, C.; Heumüller, T.; Gruber, W.; Tang, X.; Classen, A.; Schuldes, I.; Bidwell, M.; Späth, A.; Fink, R. H.; Unruh, T.; McCulloch, I.; Li, N.; Brabec, C. J. *Nature Communications* **2018**, *9*.

(142) Kietzke, T.; Neher, D.; Landfester, K.; Montenegro, R.; Güntner, R.; Scherf, U. *Nature Materials* **2003**, *2*, 408.

(143) Armleder, J.; Strunk, T.; Symalla, F.; Friederich, P.; Enrique Olivares Peña, J.; Neumann, T.; Wenzel, W.; Fediai, A. *Journal of Chemical Theory and Computation* **2021**, *17*, 3727.

(144) M. Wallace, A.; C. Fortenberry, R. *Physical Chemistry Chemical Physics* **2021**, *23*, 24413.

(145) Piquemal, J.-P.; Perera, L.; Cisneros, G. A.; Ren, P.; Pedersen, L. G.; Darden, T. A. *The Journal of Chemical Physics* **2006**, *125*, 054511.

(146) Ponder, J. W.; Wu, C.; Ren, P.; Pande, V. S.; Chodera, J. D.; Schnieders, M. J.; Haque, I.; Mobley, D. L.; Lambrecht, D. S.; Distasio, R. A.; Head-Gordon, M.; Clark, G. N. I.; Johnson, M. E.; Head-Gordon, T. *The Journal of Physical Chemistry B* **2010**, *114*, 2549.

(147) Xu, T.; Wang, W.; Yin, S. *Journal of Chemical Theory and Computation* **2018**, *14*, 3728.

(148) Bader, R. F. W. *The Journal of Physical Chemistry A* **2007**, *111*, 7966.

(149) Stone, A. J. *Chemical Physics Letters* **1981**, *83*, 233.

(150) Norton, J. E.; BréDas, J.-L. *Journal of the American Chemical Society* **2008**, *130*, 12377.

(151) Wang, L.; Kalyanaraman, C.; McCoy, A. B. *J. Chem. Phys.* **1999**, *110*, 11221.

(152) Wang, L.; Billing, G. D. *J. Phys. Chem.* **1993**, *97*, 2523.

(153) Ren, P.; Ponder, J. W. *Journal of Computational Chemistry* **2002**, *23*, 1497.

(154) Ren, P.; Wu, C.; Ponder, J. W. *Journal of Chemical Theory and Computation* **2011**, *7*, 3143.

(155) Thole, B. T. *Chemical Physics* **1981**, *59*, 341.

(156) Stone, A. J.; Alderton, M. *Molecular Physics* **1985**, *56*, 1047.

(157) Cohen, A. J.; Tantirungrotechai, Y. *Chemical Physics Letters* **1999**, *299*, 465.

(158) Xu, T.; Yin, S. *Science China Chemistry* **2014**, *57*, 1375.

(159) Rackers, J. A.; Wang, Z.; Lu, C.; Laury, M. L.; Lagardère, L.; Schnieders, M. J.; Piquemal, J.-P.; Ren, P.; Ponder, J. W. *Journal of Chemical Theory and Computation* **2018**, *14*, 5273.

(160) Yanai, T.; Tew, D. P.; Handy, N. C. *Chemical Physics Letters* **2004**, *393*, 51.

(161) Frisch, M. J.; Trucks, G. W.; Schlegel, H. B.; Scuseria, G. E.; Robb, M. A.; Cheeseman, J. R.; Scalmani, G.; Barone, V.; Petersson, G. A.; Nakatsuji, H.; Li, X.; Caricato, M.; Marenich, A. V.; Bloino, J.; Janesko, B. G.; Gomperts, R.; Mennucci, B.; Hratchian, H. P.; Ortiz, J. V.; Izmaylov, A. F.; Sonnenberg, J. L.; Williams; Ding, F.; Lipparini, F.; Egidi, F.; Goings, J.; Peng, B.; Petrone, A.; Henderson, T.; Ranasinghe, D.; Zakrzewski, V. G.; Gao, J.; Rega, N.; Zheng, G.; Liang, W.; Hada, M.; Ehara, M.; Toyota, K.; Fukuda, R.; Hasegawa, J.; Ishida, M.; Nakajima, T.; Honda, Y.; Kitao, O.; Nakai, H.; Vreven, T.; Throssell, K.; Montgomery Jr., J. A.; Peralta, J. E.; Ogliaro, F.; Bearpark, M. J.; Heyd, J. J.; Brothers, E. N.; Kudin, K. N.; Staroverov, V. N.; Keith, T. A.; Kobayashi, R.; Normand, J.; Raghavachari, K.; Rendell, A. P.; Burant, J. C.; Iyengar, S. S.; Tomasi, J.; Cossi, M.; Millam, J. M.; Klene, M.; Adamo, C.; Cammi, R.; Ochterski, J. W.; Martin, R. L.; Morokuma, K.; Farkas, O.; Foresman, J. B.; Fox, D. J. Wallingford, CT, 2016.

(162) M. J. Frisch, G. W. T., H. B. Schlegel, G. E. Scuseria, M. A. Robb, J. R. Cheeseman, G. Scalmani, V. Barone, G. A. Petersson, H. Nakatsuji, X. Li, M. Caricato, A. V. Marenich, J. Bloino, B. G. Janesko, R. Gomperts, B. Mennucci, H. P. Hratchian, J. V. Ortiz, A. F. Izmaylov, J. L. Sonnenberg, D. Williams-Young, F. Ding, F. Lipparini, F. Egidi, J. Goings, B. Peng, A. Petrone, T. Henderson, D. Ranasinghe, V. G. Zakrzewski, J. Gao, N. Rega, G. Zheng, W. Liang, M. Hada, M. Ehara, K. Toyota, R. Fukuda, J. Hasegawa, M. Ishida, T. Nakajima, Y. Honda, O. Kitao, H. Nakai, T. Vreven, K. Throssell, J. A. Montgomery, Jr., J. E. Peralta, F. Ogliaro, M. J. Bearpark, J. J. Heyd, E. N. Brothers, K. N. Kudin, V. N. Staroverov, T. A. Keith, R. Kobayashi, J. Normand, K. Raghavachari, A. P. Rendell, J. C. Burant, S. S. Iyengar, J. Tomasi, M. Cossi, J. M. Millam, M.

Klene, C. Adamo, R. Cammi, J. W. Ochterski, R. L. Martin, K. Morokuma, O. Farkas, J. B. Foresman, and D. J. Fox; C.01, R., Ed.; Gaussian, Inc: Wallingford CT, 2016.

(163) Jensen, F. *Journal of Chemical Theory and Computation* **2010**, *6*, 2726.